[8] Caligiuri MA, Briesewitz R, Yu J, Wang L, Wei M, Arnoczky KJ, et al. Novel c-CBL and CBL-b ubiquitin ligase mutations in human acute myeloid leukemia. Blood 2007;110:1022–4.
[9] Sargin B, Choudhary C, Crosetto N, Schmidt MH, Grundler R, Rensinghoff M, et al. Flt3-dependent transformation by inactivating c-Cbl mutations in AML. Blood 2007;110:1004–12.
[10] Perez B, Mechinaud F, Galambrun C, Ben Romdhane N, Isidor B, Philip N, et al. Germline mutations of the CBL gene define a new genetic syndrome with predisposition to juvenile myelomonocytic leukaemia. J Med Genet 2010;47:686–91.
[11] Niemeyer CM, Kang MW, Shin DH, Furlan I, Erlacher M, Bunin NJ, et al. Germline CBL mutations cause developmental abnormalities and predispose to juvenile myelomonocytic leukemia. Nat Genet 2010;42:794–800.
[12] Martinelli S, De Luca A, Stellacci E, Rossi C, Checquolo S, Lepri F, et al. Heterozygous germline mutations in the CBL tumor-suppressor gene cause a Noonan syndrome-like phenotype. Am J Hum Genet 2010;87:250–7.
[13] Aoki Y, Niihori T, Narumi Y, Kure S, Matsubara Y. The RAS/MAPK syndromes: novel roles of the RAS pathway in human genetic disorders. Hum Mutat 2008;29:992–1006.
[14] Tidyman WE, Rauen KA. The RASopathies: developmental syndromes of Ras/MAPK pathway dysregulation. Curr Opin Genet Dev 2009;19:230–6.
[15] Gondek LP, Tiu R, Haddad AS, O'Keefe CL, Sekeres MA, Theil KS, et al. Single nucleotide polymorphism arrays complement metaphase cytogenetics in detection of new chromosomal lesions in MDS. Leukemia 2007;21:2058–61.
[16] Kurooka H, Kuroda K, Honjo T. Roles of the ankyrin repeats and C-terminal region of the mouse notch1 intracellular region. Nucleic Acids Res 1998;26:5448–55.
[17] Kato H, Sakai T, Tamura K, Minoguchi S, Shirayoshi Y, Hamada Y, et al. Functional conservation of mouse Notch receptor family members. FEBS Lett 1996;395:221–4.
[18] Komatsuzaki S, Aoki Y, Niihori T, Okamoto N, Hennekam RC, Hopman S, et al. Mutation analysis of the SHOC2 gene in Noonan-like syndrome and in hematologic malignancies. J Hum Genet 2010;55:801–9.
[19] Weng AP, Ferrando AA, Lee W, Morris JP, Silverman LB, Sanchez-Irizarry C, et al. Activating mutations of NOTCH1 in human T cell acute lymphoblastic leukemia. Science 2004;306:269–71.
[20] O'Neil J, Grim J, Strack P, Rao S, Tibbitts D, Winter C, et al. FBW7 mutations in leukemic cells mediate NOTCH pathway activation and resistance to gamma-secretase inhibitors. J Exp Med 2007;204:1813–24.
[21] Thompson BJ, Jankovic V, Gao J, Buonamici S, Vest A, Lee JM, et al. Control of hematopoietic stem cell quiescence by the E3 ubiquitin ligase Fbw7. J Exp Med 2008;205:1395–408.
[22] Maser RS, Choudhury B, Campbell PJ, Feng B, Wong KK, Protopopov A, et al. Chromosomally unstable mouse tumours have genomic alterations similar to diverse human cancers. Nature 2007;447:966–71.
[23] Rocquain J, Carbuccia N, Trouplin V, Raynaud S, Murati A, Nezri M, et al. Combined mutations of ASXL1, CBL, FLT3, IDH1, IDH2, JAK2, KRAS, NPM1, NRAS, RUNX1, TET2 and WT1 genes in myelodysplastic syndromes and acute myeloid leukemias. BMC Cancer 2010;10:401.
[24] Gille H, Kortenjann M, Thomae O, Moomaw C, Slaughter C, Cobb MH, et al. ERK phosphorylation potentiates Elk-1-mediated ternary complex formation and transactivation. EMBO J 1995;14:951–62.
[25] Barr RK, Bogoyevitch MA. The c-Jun N-terminal protein kinase family of mitogen-activated protein kinases (JNK MAPKs). Int J Biochem Cell Biol 2001;33:1047–63.
[26] Shiba N, Park MJ, Taki T, Takita J, Hiwatari M, Kanazawa T, et al. CBL mutations in infant acute lymphoblastic leukaemia. Br J Haematol 2012;156:672–4.
[27] Nicholson L, Knight T, Matheson E, Minto L, Case M, Sanichar M, et al. Casitas B lymphoma mutations in childhood acute lymphoblastic leukemia. Genes Chromosomes Cancer 2012;51:250–6.
[28] Jehn BM, Dittert I, Beyer S, von der Mark K, Bielke W. c-Cbl binding and ubiquitin-dependent lysosomal degradation of membrane-associated Notch1. J Biol Chem 2002;277:8033–40.
[29] Checquolo S, Palermo R, Cialfi S, Ferrara G, Oliviero C, Talora C, et al. Differential subcellular localization regulates c-Cbl E3 ligase activity upon Notch3 protein in T-cell leukemia. Oncogene 2010;29:1463–74.
[30] Ogawa S, Shih LY, Suzuki T, Otsu M, Nakauchi H, Koeffler HP, et al. Deregulated intracellular signaling by mutated c-CBL in myeloid neoplasms. Clin Cancer Res 2010;16:3825–31.
[31] Lo FY, Tan YH, Cheng HC, Salgia R, Wang YC. An E3 ubiquitin ligase: c-Cbl: a new therapeutic target of lung cancer. Cancer 2011;117:5344–50.
[32] van Noort M, Clevers H. TCF transcription factors, mediators of Wnt-signaling in development and cancer. Dev Biol 2002;244:1–8.
[33] Gutierrez A, Sanda T, Ma W, Zhang J, Grebliunaite R, Dahlberg S, et al. Inactivation of LEF1 in T-cell acute lymphoblastic leukemia. Blood 2010;115:2845–51.
[34] Ruas M, Peters G. The p16INK4a/CDKN2A tumor suppressor and its relatives. Biochim Biophys Acta 1998;1378:F115–77.

RESIDENT & FELLOW SECTION

Section Editor
Mitchell S.V. Elkind, MD, MS

Clinical Reasoning: A young man with progressive subcortical lesions and optic nerve atrophy

Shoko Komatsuzaki, MD, PhD
Osamu Sakamoto, MD, PhD
Nobuo Fuse, MD, PhD
Mitsugu Uematsu, MD, PhD
Yoichi Matsubara, MD
Toshihiro Ohura, MD, PhD

Correspondence & reprint requests to Dr. Komatsuzaki: komatsuzaki@med.tohoku.ac.jp

SECTION 1

The male patient is the third child of unrelated Japanese parents. His older sister had tachypnea and feeding difficulties, and died at 5 days of age. The patient was delivered at term (birthweight, 3.8 kg), following an unremarkable pregnancy. He presented with tachypnea, metabolic acidosis, and hyperammonemia (944 μmol $\cdot$ L^{-1}) at 6 days.

Questions for consideration:

1. What is the differential for infantile presentation of hyperammonemia in the neonatal period?
2. What laboratory tests would you pursue?

GO TO SECTION 2

From the Departments of Medical Genetics (S.K., Y.M.) and Pediatrics (O.S., M.U., T.O.), Tohoku University School of Medicine, Sendai; Department of Ophthalmology (N.F.), Tohoku University Graduate School of Medicine, Sendai; and Department of Pediatrics (T.O.), Sendai City Hospital, Sendai, Japan.

Go to Neurology.org for full disclosures. Disclosures deemed relevant by the authors, if any, are provided at the end of this article.

SECTION 2

Hyperammonemia occurs in urea cycle disorders (e.g., ornithine transcarbamylase deficiency) and organic acidurias (e.g., methylmalonic aciduria, propionic aciduria, and isovaleric aciduria) and fatty acid oxidation defects (e.g., multiple acyl-CoA dehydrogenase deficiency). The existence of acidosis with ketosis indicates organic aciduria, whereas respiratory alkalosis is observed in urea cycle defects. Diagnosis is based on quantitative assay of amino acids and acylcarnitines from dried blood and organic acids in urine samples.

Case: part 2. Elevated levels of 2-methylcitric acid and 3-hydroxypropionic acid were found in the urine. The plasma propionic acid concentration was increased (4.5 $mg \cdot dL^{-1}$), and propionyl-CoA carboxylase (PCC) activity in fibroblasts was decreased (6.3 $pmol \cdot min^{-1} \cdot mg^{-1}$ protein, normal value: 292 [n = 4]). The patient was treated with exchange transfusion, peritoneal dialysis, high-calorie infusions, and a low-protein diet.

Questions for consideration:

1. What is the diagnosis?
2. How should these infants be treated in the acute period?
3. What treatment should be given long term?

GO TO SECTION 3

Propionic aciduria is an autosomal recessive disease caused by a deficiency of PCC. PCC is a biotin-dependent enzyme that catalyzes the branched chain amino acids valine and isoleucine but not leucine; it also catalyzes methionine, threonine, and odd-chain fatty acids in the mitochondrial matrix. PCC is composed of α and β subunits, which are encoded by nuclear genes *PCCA* and *PCCB*, respectively. PCC deficiency causes accumulation of propionic acid, 3-hydroxypropionic acid, 2-methylcitric acid, and propionylglycine in blood, urine, and CSF.[1]

Clinical forms of propionic aciduria are described on the basis of the age at onset: neonatal and late onset. The neonatal-onset form is characterized by poor sucking, vomiting, failure to thrive, and progressive encephalopathy. Routine laboratory findings are metabolic acidosis, ketosis, lactic acidosis, hyperammonemia, leukocytopenia, thrombocytopenia, and anemia. The late-onset form is characterized by periodic vomiting to life-threatening hyperammonemia, psychomotor retardation, and other chronic symptoms.[1] Propionic aciduria is characterized by increased excretion of propionic acid, 3-hydroxy propionic acid, and 2-methylcitric acid in urine as well as elevated concentrations of propionyl-carnitine in blood serum or plasma. It is initially diagnosed based on enzymatic analysis of propionyl-CoA carboxylase activity in fibroblasts or leukocytes. Identification of the specific mutations in *PCCA* or *PCCB* is required to confirm the diagnosis.[1]

The increased 2-methylcitric acid and 3-hydroxypropionic acid levels and decreased propionyl-CoA carboxylase activity in this case indicated propionic aciduria. Mutation analysis revealed homozygosity for p.Thr428Ile in the *PCCB* gene, confirming propionic aciduria.

Emergency treatment for propionic aciduria involves low-protein, high-energy nutrition and rehydration. Almost all propionic aciduria patients show hyperammonemia, which results from inhibition of urea cycle enzymes by accumulated acyl-CoA esters. Some patients, especially those severely affected, require hemodialysis/hemofiltration. Sodium benzoate and carbamyl glutamate are used to treat secondary hyperammonemia.[2] Long-term management comprises low-protein diet and carnitine supplementation. Arginine and carnitine are administered for detoxification of toxic metabolites. Metronidazole is often administered to reduce production of propionic acid by gut bacteria.[1]

Case: part 3. After emergency intervention, the patient was treated with a low-protein diet and carnitine supplementation. During the first 5 years of life, he had several episodes of metabolic acidosis requiring hospitalization; however, he never showed metabolic decompensation thereafter. Despite nearly normal development at 4 years, he thereafter developed intellectual deficits that gradually deteriorated with age: his developmental quotient was 88 at the age of 4 and 74 at 6, while his IQ was 73 at the age of 7 and 54 at 15.

At 22 years, metronidazole administration was initiated to reduce propionic acid production by gut bacteria. Bilateral vision impairment was also detected during a regular health check-up. Ophthalmologic examination showed temporal pallor of the right eye and left optic nerve atrophy (figure 1). The patient's visual acuity was 20/200 in the right eye and 20/300 in the left eye. In both eyes, his visual fields showed central scotoma, and his visual evoked potential (VEP) displayed decreased amplitude. An electroretinogram showed normal findings, while optical coherence tomography revealed no retinal structure abnormalities. Within a year, his visual acuity decreased from 20/200 to hand motion in the right eye and from 20/300 to counting fingers in the left. He also had intention tremor, mild hyperammonemia, and elevated lactic acid levels, but no metabolic acidosis. Ophthalmologic examination results at 11 years were normal.

Brain MRI revealed symmetric lesions of the basal ganglia, including the caudate nucleus, putamen, and globus pallidus (figure 2A). At 23 years, no symptoms were present, but diffusion-weighted MRI of the brain showed subcortical lesions (figure 2, B–D). At 24 years, he showed acute reversible muscle weakness and dysarthria, comparable to pseudobulbar paralysis. Neurologic evaluation showed increased deep tendon reflexes on the left side of the body, while subsequent MRI of the brain revealed progression of the subcortical lesions (figure 2, E–G), without evidence of metabolic decompensation.

Figure 1 Fundal images

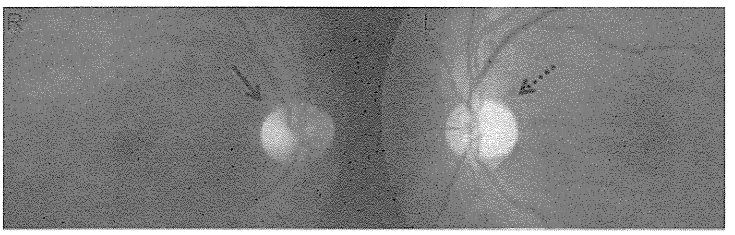

Temporal pallor in the right eye and optic nerve atrophy in the left.

Figure 2 MRI

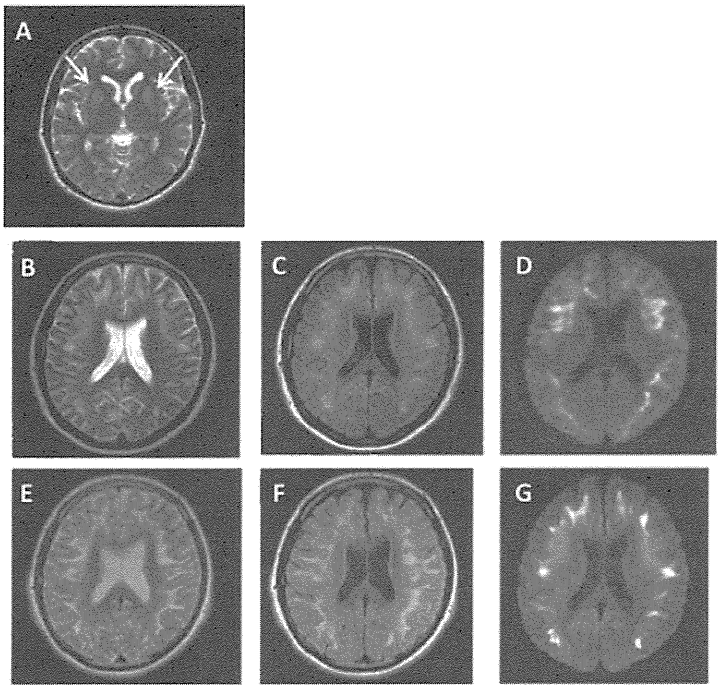

(A, B, E) T2-weighted images; the arrows in A indicate the high intensity of basal ganglia areas. (C, F) Fluid-attenuated inversion recovery. (D, G) Diffusion-weighted imaging, showing abnormal signals in subcortical lesions.

At 24 years, chest radiography showed an increased cardiothoracic ratio (65%) and pulmonary edema. Echocardiogram showed dilated hypokinetic left ventricle and a decrease in ejection fraction (48%), resembling dilated cardiomyopathy. The patient was administered furosemide, spironolactone, and carvedilol.

Questions for consideration:

1. Why did this patient's condition deteriorate even without metabolic acidosis crises?
2. What is the range of prognosis for neonatal-onset form propionic aciduria?
3. What type of monitoring will he need?

GO TO SECTION 4

SECTION 4

The accumulation of toxic organic acids causes cerebral stroke that cannot be accounted for by hypoxemia or vascular insufficiency: this neurologic event is termed metabolic stroke.[3] Toxic metabolites cause secondary mitochondrial dysfunction, which leads to metabolic stroke.[4] According to the recent "trapping hypothesis," the limited transport of toxic metabolites from the brain to the blood compartment leads to accumulation of toxic dicarboxylic acids in glutaric aciduria type I and methylmalonic aciduria.[5] Like propionic aciduria, methylmalonic aciduria is also a branched-chain amino acid disorder. For propionic aciduria patients, accumulation of the dicarboxylic acid 2-methylcitric acid seems likely; however, it has not yet been sufficiently documented.

Patients with propionic aciduria and methylmalonic aciduria often present with mental retardation, epilepsy, and extrapyramidal symptoms. Sixty percent of patients with propionic aciduria have an IQ lower than 75.[2] Symmetric lesions of the basal ganglia are the most frequently reported MRI changes in propionic aciduria and methylmalonic aciduria.[2] Subcortical white matter abnormality was additionally reported in 11.5% of patients with methylmalonic aciduria.[6] However, these findings have not been confirmed in propionic aciduria, probably because the number of patients is relatively small.

Compared to previously reported late-onset optic nerve atrophy in patients with methylmalonic aciduria and propionic aciduria,[7] our patient is the oldest. The previous report suggested that optic nerve atrophy observed in propionic aciduria and methylmalonic aciduria resembled Leber hereditary optic neuropathy (LHON),[7] as both showed optic nerve atrophy and normal retina. LHON is caused by 1 of 3 pathogenic mtDNA mutations at the nucleotide positions 11,778, 3,460, and 14,484, located in genes encoding the mitochondrial complex I subunits. Our patient carried none of these mutations. The common findings between optic nerve atrophy in propionic aciduria/methylmalonic aciduria and LHON suggest that secondary mitochondrial dysfunction leads to optic nerve atrophy in patients with propionic aciduria and methylmalonic aciduria. Optic nerve atrophy is age-dependent, but independent of metabolic control, other neurologic complications, and overall health status.[7] Therefore, we recommend regular ophthalmologic examination of patients with propionica aciduria and methylmalonic aciduria.

In many countries, propionic aciduria is targeted in newborn screening programs. About 60% of patients diagnosed through newborn screening were already symptomatic and less than 10% remained asymptomatic.[8] Even though newborn screening diagnosis does not positively correlate with a milder clinical course or better neurologic outcome,[8] it is important from the viewpoint of earlier diagnosis and decreased early mortality.

According to genotype and phenotype correlation analysis, certain null mutations are related to neonatal onset, while certain missense mutations are related to the late-onset form.[9] Although late-onset patients have higher survival rates compared to neonatal-onset patients,[9] both face the risk of relapses of life-threatening episodes of metabolic decompensation and risk of death or further neurologic damage.

PCC plays a role mainly in the liver; therefore, liver transplantation has been considered an alternative therapy.[2] Liver transplantation minimizes further metabolic acidosis and improves the quality of life. However, various complications, including basal ganglia lesions, cardiomyopathy, and optic nerve atrophy, were reported in patients without metabolic decompensation.[2,7] Even after liver transplantation, stroke-like episodes or cardiomyopathy was reported.[10]

Thus, conventional management is insufficient to improve the long-term prognosis for propionic aciduria patients, indicating the need for novel therapeutic approaches based on a better understanding of the pathophysiology.

AUTHOR CONTRIBUTIONS

Shoko Komatsuzaki contributed to conceptualizing the study and design, analysis and interpretation of data, drafting/revising the manuscript. Osamu Sakamoto contributed to the analysis and interpretation of the data, drafting/revising the manuscript. Nobuo Fuse contributed to the analysis and interpretation of data, drafting/revising the manuscript. Mitsugu Uematsu contributed to the analysis and interpretation of data, drafting/revising the manuscript. Yoichi Matsubara contributed to drafting/revising the manuscript. Toshihiro Ohura contributed in critical review of the manuscript, reviewed the literature for manuscript preparation, and supervised the clinical management of study patients.

ACKNOWLEDGMENT

The authors thank Professor Shigeo Kure and Dr. Shuhei Kakizaki at the Department of Pediatrics, Tohoku University, for collection of the patients' clinical data and comments on the manuscript; and Professor Stefan Koelker and Dr. Sven Sauer at Children's Hospital Heidelberg for their comments on the manuscript.

DISCLOSURE

The authors report no disclosures relevant to the manuscript. **Go to Neurology.org for full disclosures.**

REFERENCES

1. Fenton WA, Gravel RA, Rosenblatt DS. Disorders of propionate and methylmalonate metabolism. In: Scrver CR, Beaudet AL, Sly WS, Valle D, eds. The Metabolic and Molecular Bases of Inherited Metabolic Disease. New York: McGraw-Hill; 2001:2165–2193.
2. de Baulny HO, Benoist JF, Rigal O, Touati G, Rabier D, Saudubray JM. Methylmalonic and propionic acidaemias: management and outcome. J Inherit Metab Dis 2005;28: 415–423.

3. Heidenreich R, Natowicz M, Hainline BE, et al. Acute extrapyramidal syndrome in methylmalonic acidemia: "metabolic stroke" involving the globus pallidus. J Pediatr 1988;113:1022–1027.
4. Schwab MA, Sauer SW, Okun JG, et al. Secondary mitochondrial dysfunction in propionic aciduria: a pathogenic role for endogenous mitochondrial toxins. Biochem J 2006;398:107–112.
5. Sauer SW, Opp S, Mahringer A, et al. Glutaric aciduria type I and methylmalonic aciduria: simulation of cerebral import and export of accumulating neurotoxic dicarboxylic acids in in vitro models of the blood-brain barrier and the choroid plexus. Biochim Biophys Acta 2010;1802:552–560.
6. Radmanesh A, Zaman T, Ghanaati H, Molaei S, Robertson RL, Zamani AA. Methylmalonic acidemia: brain imaging findings in 52 children and a review of the literature. Pediatr Radiol 2008;38:1054–1061.
7. Williams ZR, Hurley PE, Altiparmak UE, et al. Late onset optic neuropathy in methylmalonic and propionic acidemia. Am J Ophthalmol 2009;147:929–933.
8. Grunert SC, Mullerleile S, de Silva L, et al. Propionic acidemia: neonatal versus selective metabolic screening. J Inherit Metab Dis 2012;35:41–49.
9. Perez-Cerda C, Merinero B, Rodriguez-Pombo P, et al. Potential relationship between genotype and clinical outcome in propionic acidaemia patients. Eur J Hum Genet 2000;8:187–194.
10. Collins J, Kelly D. Cardiomyopathy in propionic acidemia. Eur J Pediatr 1994;153:53.

Novel Insights from Clinical Practice

HORMONE RESEARCH IN PÆDIATRICS

Horm Res Paediatr 2014;81:139–144
DOI: 10.1159/000355380

Received: July 12, 2013
Accepted: August 30, 2013
Published online: November 20, 2013

De novo Frameshift Mutation in *Fibroblast Growth Factor 8* in a Male Patient with Gonadotropin Deficiency

Erina Suzuki[a] Shuichi Yatsuga[d] Maki Igarashi[a] Mami Miyado[a] Kazuhiko Nakabayashi[b] Keiko Hayashi[b] Kenichirou Hata[b] Akihiro Umezawa[c] Gen Yamada[e] Tsutomu Ogata[a, f] Maki Fukami[a]

Departments of [a]Molecular Endocrinology and [b]Maternal-Fetal Biology, National Research Institute for Child Health and Development, [c]Department of Reproductive Biology, Center for Regenerative Medicine, National Research Institute for Child Health and Development, Tokyo, [d]Department of Pediatrics and Child Health, Kurume University School of Medicine, Kurume, [e]Department of Developmental Genetics, Institute of Advanced Medicine, Wakayama Medical University, Wakayama, and [f]Department of Pediatrics, Hamamatsu University School of Medicine, Hamamatsu, Japan

Established Facts

- Missense, nonsense, and splice mutations in *Fibroblast Growth Factor 8 (FGF8)* have been identified in patients with hypothalamo-pituitary dysfunction and craniofacial anomalies.

Novel Insights

- *FGF8* frameshift mutations account for a part of the etiology of hypothalamo-pituitary dysfunction and craniofacial anomalies.
- Micropenis in patients with *FGF8* mutations can be ascribed to gonadotropin deficiency and impaired outgrowth of the anlage of the penis.

Key Words
Fibroblast Growth Factor 8 · Frameshift mutation · Gonadotropin deficiency · Hypothalamo-pituitary dysfunction

Abstract

Background/Aims: Missense, nonsense, and splice mutations in the *Fibroblast Growth Factor 8 (FGF8)* have recently been identified in patients with hypothalamo-pituitary dysfunction and craniofacial anomalies. Here, we report a male patient with a frameshift mutation in *FGF8*. ***Case Report:*** The patient exhibited micropenis, craniofacial anomalies, and ventricular septal defect at birth. Clinical evaluation at 16 years and 8 months of age revealed delayed puberty, hyposmia, borderline mental retardation, and mild hearing difficulty. Endocrine findings included gonadotropin deficiency and primary hypothyroidism. ***Results:*** Molecular analysis identified a de novo heterozygous p.S192fsX204 mutation in the last exon of *FGF8*. RT-PCR analysis of normal human tissues detected *FGF8* expression in the genital skin, and whole-mount in situ hybridization analysis of mouse embryos revealed *Fgf8* expression in the anlage of the penis. ***Conclusion:*** The results indicate that frameshift mutations in *FGF8* account for a part of the etiology of hypothalamo-pituitary dysfunction. Micropenis in patients with *FGF8* abnormalities appears to be caused by gonadotropin deficiency and defective outgrowth of the anlage of the penis.

E. Suzuki, S. Yatsuga and M. Igarashi contributed equally to this work.

KARGER

E-Mail karger@karger.com
www.karger.com/hrp

1663–2818/13/0812–0139$38.00/0

Maki Fukami, MD
Department of Molecular Endocrinology
National Research Institute for Child Health and Development
2-10-1 Ohkura, Setagaya, Tokyo 157-8535 (Japan)
E-Mail fukami-m@ncchd.go.jp

Introduction

Fibroblast growth factor (FGF) 8 (FGF8, NP_149353.1) is the major ligand of FGF receptor 1 (FGFR1) and plays a critical role in formation of the anterior midline in the forebrain [1–5]. Animal studies have indicated that FGF8 regulates the development of GnRH neurons in a dose-dependent manner [4, 5]. Recently, multiple missense mutations as well as two nonsense and one splice mutation in *FGF8* (NM_033163.3) have been identified in patients with various types of hypothalamo-pituitary dysfunction and craniofacial anomalies [1, 3, 4–9]. The mutation-positive patients invariably manifest gonadotropin deficiency and/or delayed puberty, indicating that GnRH neurons are highly vulnerable to impaired function of FGF8 [1, 3, 4–9]. Furthermore, mutations in several genes involved in the FGF8–FGFR1 network have been shown to underlie gonadotropin deficiency [1].

However, given the small number of reported patients, further studies are necessary to clarify the mutation spectrum and phenotypes of *FGF8* abnormalities. For example, frameshift mutations in *FGF8* have not been identified, and the underlying mechanisms of genital anomalies in patients with *FGF8* mutations have poorly been investigated. Here, we report a male patient with a de novo frameshift mutation in *FGF8*.

Subjects and Methods

Case Report

The male patient was born to non-consanguineous Japanese parents at 38 weeks' gestation. At birth, the patient manifested micropenis, phimosis, and hypoplastic scrotum. He also exhibited cleft lip and palate, strabismus, and ventricular septal defect. Hypospadias and cryptorchidism were absent. From 6 months of age, he underwent surgical interventions for facial and genital abnormalities. He had multiple episodes of convulsions from 12 years of age, and was treated with anticonvulsants. From infancy to early teens, his stature followed the –2.0 SD growth curve for Japanese males (fig. 1a).

At 16 years and 8 months of age, the patient was referred to our clinic for delayed puberty. Clinical assessment revealed a high-pitched voice and pubic and axillary hair of Tanner stage 1–2. His penile length was 1.5 cm (fig. 1b). Bilateral testes of ~1 ml were palpable in the scrotum. His stature and weight were 154.0 cm (–2.8 SD) and 52.9 kg (–0.8 SD), respectively. He had mild hearing difficulty and borderline mental retardation with a WISC-III IQ score of 71. Although he showed a response to a smell test using intravenous injection of combined vitamins (Alinamin; Takeda Pharmaceutical Co. Ltd, Osaka, Japan), he was unable to identify various odorants. Thus, he was suspected as having hyposmia. Brain magnetic resonance imaging delineated no structural abnormalities in the hypothalamus, pituitary, or olfactory bulbs (fig. 1b). The patient manifested no symptoms associated with the heart anomaly, although cardiac evaluation showed a ventricular septal defect of approximately 2 mm. His father, mother and elder brother were clinically normal, and had heights of 164 cm (–1.2 SD), 143 cm (–2.7 SD), and 167 cm (–0.7 SD), respectively.

Endocrine examinations indicated multiple hormone deficiencies in the patient (table 1). Blood LH values were low at baseline and poorly responded to GnRH stimulation. FSH values were low-normal. Slightly elevated TSH levels and mildly decreased free T_4 levels indicated primary hypothyroidism. The IGF-1 level was low-normal. Blood levels of prolactin, ACTH, and cortisol were within the normal range. Anti-thyroperoxidase and anti-thyroglobulin antibodies were negative. Thyroid technetium-99m scintigram revealed no abnormalities. After initiation of levothyroxine supplementation therapy (50 μg/day), TSH and free T_4 values remained within the normal range.

Mutation Analysis

This study was approved by the Institutional Review Board Committee at the National Center for Child Health and Development and performed after obtaining written informed consent. A genomic DNA sample from the patient was analyzed for mutations in 13 genes that have been implicated in gonadotropin deficiency: *FGFR1*, *KAL1*, *FGF8*, *PROK2*, *PROKR2*, *TAC3*, *TACR3*, *KISS1*, *KISS1R*, *GNRHR*, *GNRH1*, *CHD7*, and *NELF* [1, 7, 10, 11]. Mutations were screened by the Haloplex method (Agilent Technologies, Palo Alto, Calif., USA) on a MiSeq next-generation sequencer (Illumina, San Diego, Calif., USA). An *FGF8* mutation indicated by the screening analysis was confirmed by Sanger sequencing with primers, 5′-GCGAGTTGTGAGGGATTAGAGA-3′ and 5′-GGGTGCCCTACAGGATGAG-3′. To verify the heterozygous mutation, the PCR product was subcloned into a TOPO TA cloning vector (Life Technologies, Carlsbad, Calif., USA) and the mutant and wild-type alleles were sequenced separately. Genomic DNA samples from the parents and brother were examined for the presence or absence of the *FGF8* mutation.

Expression Analysis for FGF8/Fgf8 in Normal Human Tissues and Mouse Embryos

We investigated mRNA expression of *FGF8* in normal human tissues by PCR. Human cDNA samples were purchased from Clontech (Palo Alto, Calif., USA) or prepared by RT-PCR. PCR analysis of *FGF8* was performed with primers, 5′-AGTCCGAGGAGCCGAGA-3′ and 5′-AAGTGGACCTCACGCTGGT-3′. As an internal control, we amplified *GAPDH* with primers, 5′-CCACCCATGGCAAATTCCATGGCA-3′ and 5′-TCTAGACGGCAGGTCAGGTCCACC-3′.

We also examined the expression of *Fgf8* in the developing external genitalia of mouse embryos by whole-mount in situ hybridization. An antisense cRNA fragment corresponding to nucleotide 1–978 of mouse *Fgf8* (BC048734) was utilized as a probe. The procedures were performed as described previously [12].

Results

Mutation Analysis

The patient carried a heterozygous frameshift mutation in the last exon of *FGF8* (p.S192fsX204, c.574delT)

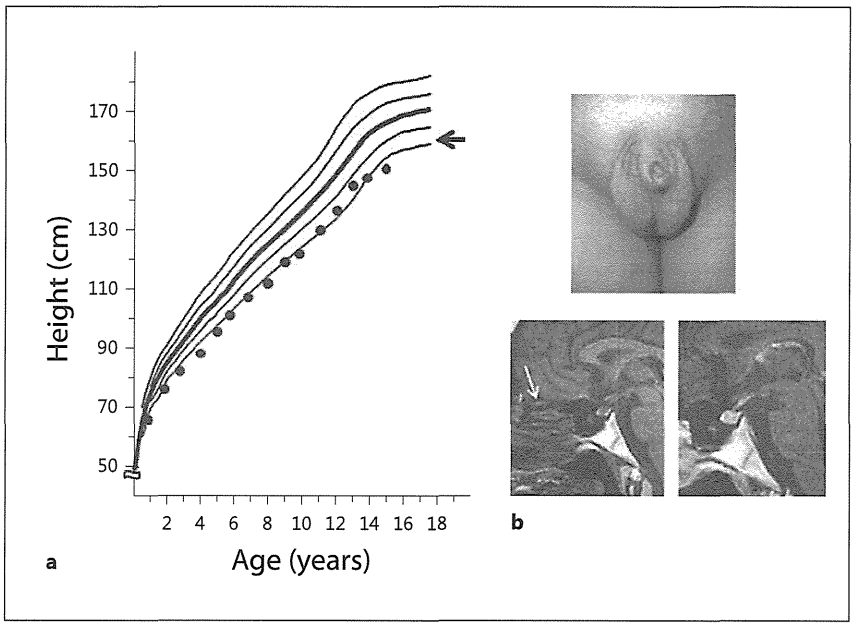

Fig. 1. Clinical findings of the patient. **a** Growth chart. Actual height of the patient is plotted against the growth curve for Japanese boys (the mean, ±1.0 SD and ±2.0 SD). The arrow indicates the midparental height. **b** Upper panel: genital appearance at 16 years and 8 months of age. Lower panels: brain magnetic resonance imaging. No abnormalities are detected in the hypothalamus, pituitary, or olfactory bulbs (arrow).

Table 1. Endocrine data of the patient

	Stimulus (dosage)	Patient		Reference values[1]	
		baseline	peak	baseline	peak
At diagnosis					
LH, mIU/ml	GnRH (100 μg)[2]	**0.5**	**4.6**	0.8–4.2	18.2–38.0
FSH, mIU/ml	GnRH (100 μg)[2]	3.0	9.5	2.9–10.8	5.8–22.3
GH, ng/ml	Insulin (3 U)[2]	0.87	**3.18**[3]	0.6–8.7	>6.0
Prolactin, ng/ml	TRH (350 μg)[2]	4.3	14.4	1.1–9.5	–
TSH, μU/ml	TRH (350 μg)[2]	*8.3*	23.0	0.6–5.9	5.8–30.6
IGF-1, ng/ml		301[4]	–	250–680	–
ACTH, pg/ml	CRH (100 μg)[2]	9.5	50.3	5.3–51.1	17.2–153.3
Cortisol, μg/dl	CRH (100 μg)[2]	8.4	25.8	3.9–21.3	13.1–35.6
Free T_4, ng/dl		**0.79**	–	1.0–1.7	–
Free T_3, pg/ml		2.8	–	2.1–4.1	–
Testosterone, ng/ml	HCG (4,000 U)[5]	**0.12**	**0.38**	2.8–7.0	11.0–13.1
On levothyroxine treatment[6]					
TSH, μU/ml		0.68	–	0.6–5.9	–
Free T_4, ng/dl		1.14	–	1.0–1.7	–

The conversion factors to the SI unit: LH, 1.0 (IU/l); FSH, 1.0 (IU/l); GH, 1.0 (μg/l); prolactin, 43.48 (pmol/l); TSH, 1.0 (mIU/l); IGF-I, 0.131 (nmol/l); ACTH, 0.22 (pmol/l); cortisol, 27.59 (nmol/l); free T_4, 12.87 (pmol/l); free T_3, 1.54 (pmol/l), and testosterone, 3.47 (nmol/l). Hormone values above the reference range are italicized and those below the reference range are boldfaced.

[1] Reference values in age-matched males. [2] GnRH, insulin and TRH i.v.; blood sampling at 0, 30, 60, 90, and 120 min. [3] Low GH values of the patient may be due to insufficient hypoglycemic stimulation; blood glucose was 89 mg/dl at 0 min, and 58 mg/dl at 30 min. [4] –1.7 SD. [5] HCG i.m. for 3 consecutive days; blood sampling on days 1 and 4. [6] Levothyroxine 50 μg/day.

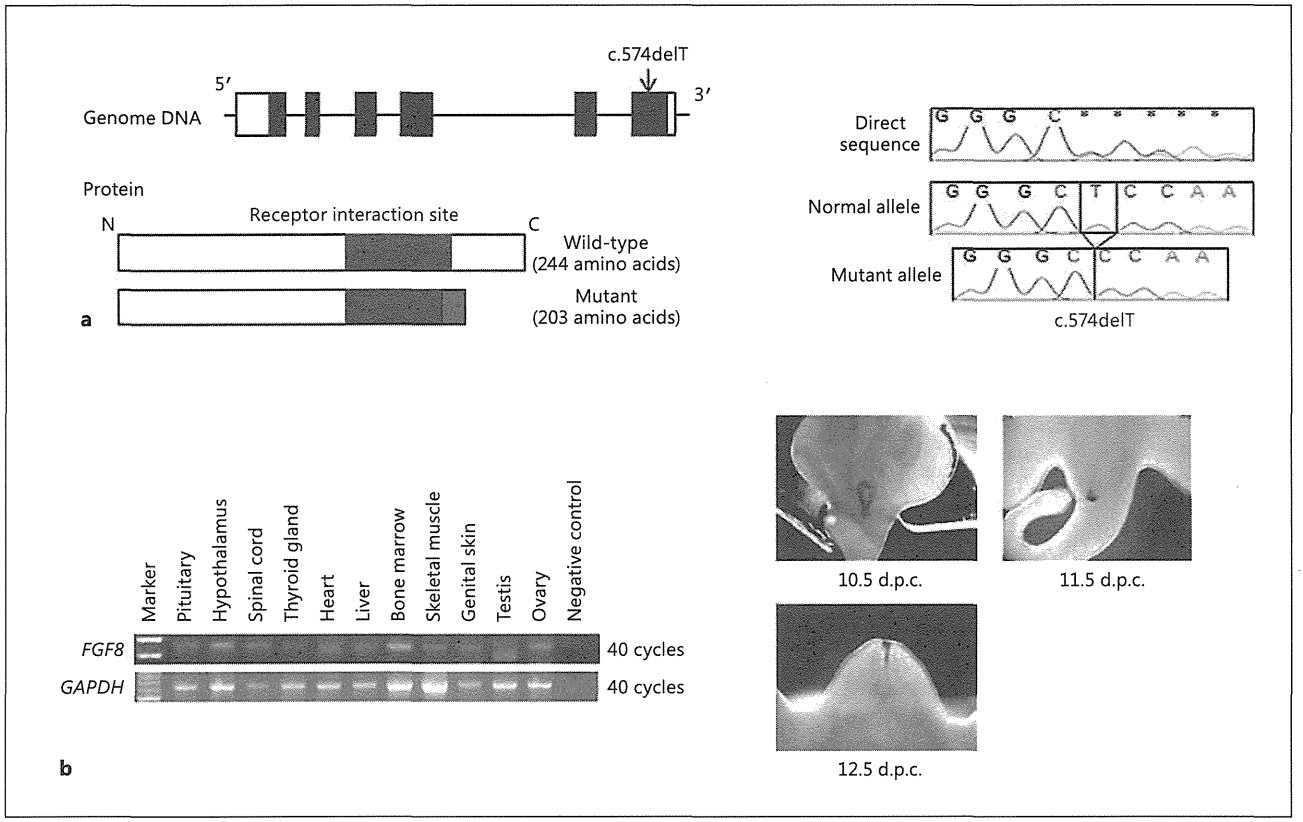

Fig. 2. Mutation analysis of *FGF8* and expression studies of *FGF8/Fgf8*. **a** *FGF8* mutation identified in the patient. The positions of nucleotides and amino acids correspond to NM_033163.3 and NP_149353.1, respectively. Left panel: the genomic and protein structures of FGF8. The white and black boxes in genome DNA indicate the non-coding and coding regions, respectively. The blue boxes in the protein depict the receptor interaction site at codons 83–207 and the red box indicates truncated amino acids. Right panel: chromatograms of the c.574delT mutation. **b** Expression analyses of *FGF8/Fgf8*. Left panel: PCR-based cDNA screening for human *FGF8*. After 40 cycles, PCR products for *FGF8* were detected in all tissues examined. *GAPDH* is utilized as an internal control. Right panel: whole-mount in situ hybridization analysis in mouse embryos. Purple signals indicate expression of mouse *Fgf8*. d.p.c. = Days post-coitum.

(fig. 2a). No pathogenic mutations were identified in other tested genes. The p.S192fsX204 mutation was predicted to truncate the C-terminus of FGF8 by replacing 53 amino acids with 12 aberrant amino acids (fig. 2a). This mutation affected a part of the receptor interacting site of FGF8 (codons 83–207). The *FGF8* mutation was not identified in the parents or brother.

Expression Analysis for FGF8/Fgf8 in Normal Human Tissues and Mouse Embryos

PCR-based cDNA screening indicated that human *FGF8* is expressed in a range of tissues including the hypothalamus, pituitary, thyroid gland, heart, and genital skin (fig. 2b). Whole-mount in situ hybridization indicated that mouse *Fgf8* is expressed in the epithelium of the outmost part of the urogenital sinus before outgrowth of the anlage of the penis (genital tubercle) (10.5 days post-coitum) and in the epithelium of distal urethral plate during development of the genital tubercle (11.5 and 12.5 days post-coitum) (fig. 2b).

Discussion

We identified a de novo *FGF8* frameshift mutation in a Japanese patient with gonadotropin deficiency and multiple complications. The p.S192fsX204 mutation resides in the last exon of *FGF8* and is likely to escape non-

sense-mediated mRNA decay [13]. However, the mutation is predicted to alter the C-terminal structure of the protein and affect the receptor interacting site. In this context, Falardeau et al. [4] indicated that a missense mutation at the 229th codon is sufficient to reduce in vitro activity. Thus, although in vitro functional assays have not been conducted for p.S192fsX204, this mutation appears to markedly impair the function of FGF8. Consistent with this, the patient manifested gonadotropin deficiency, hyposmia, and craniofacial anomalies comparable to the phenotypes of previously reported patients with nonsense, missense, and splice mutations of *FGF8* [1, 3–9]. These data indicate for the first time that frameshift mutations of *FGF8* account for a part of the etiology of hypothalamo-pituitary dysfunction and craniofacial anomalies.

We cannot exclude the possibility that the patient carries additional mutations in other genes involved in hypothalamo-pituitary function. Although *FGF8* abnormalities are known to cause gonadotropin deficiency mostly as monoallelic mutations, they can also appear in an oligogenic condition [1]. Therefore, although our patient has no mutations in the 13 known causative genes for gonadotropin deficiency, he may have mutations in other unexamined genes. Indeed, several genes including *FGF17*, *IL17RD*, *DUSP6*, *SPRY4*, and *FLRT3* have recently been implicated in gonadotropin deficiency [1].

The Japanese patient manifested severe micropenis. This phenotype is consistent with severe gonadotropin deficiency [14]. In addition, defective formation the penis during fetal period may have played a role in the development of micropenis, because outgrowth of the genital tubercle in mouse embryos primarily depends on *Fgf8* signaling [12]. Indeed, we found expression of *FGF8/Fgf8* in human genital skin and in the epithelium of the mouse genital tubercle.

The patient manifested primary hypothyroidism and a congenital heart anomaly, neither of which has been reported in patients with *FGF8* mutations. Although we detected expression of *FGF8* in the human thyroid gland and heart, and several studies have revealed that FGF8 plays an essential role in formation of the cardiovascular system and thyroid gland in mice [15–20], it remains unknown whether thyroid and heart abnormalities of the patient are associated with the *FGF8* mutation.

In summary, we identified the first frameshift *FGF8* mutations in a patient with gonadotropin deficiency. The results indicate molecular diversity of *FGF8* abnormalities.

Acknowledgements

This work was supported by grants from the Ministry of Health, Labor and Welfare and from Takeda Science Foundation, by Grant-in-Aid for Scientific Research from the Japan Society for the Promotion of Science, by Grant-in-Aid for Scientific Research on Innovative Areas from the Ministry of Education, Culture, Sports, Science and Technology and by the Grant of National Center for Child Health and Development.

Disclosure Statement

The authors have no conflicts of interest to disclose.

References

▶1 Miraoui H, Dwyer AA, Sykiotis GP, Plummer L, Chung W, Feng B, Beenken A, Clarke J, Pers TH, Dworzynski P, Keefe K, Niedziela M, Raivio T, Crowley WF Jr, Seminara SB, Quinton R, Hughes VA, Kumanov P, Young J, Yialamas MA, Hall JE, Van Vliet G, Chanoine JP, Rubenstein J, Mohammadi M, Tsai PS, Sidis Y, Lage K, Pitteloud N: Mutations in FGF17, IL17RD, DUSP6, SPRY4, and FLRT3 are identified in individuals with congenital hypogonadotropic hypogonadism. Am J Hum Genet 2013;92:725–743.

▶2 Goetz R, Ohnishi M, Ding X, Kurosu H, Wang L, Akiyoshi J, Ma J, Gai W, Sidis Y, Pitteloud N, Kuro-O M, Razzaque MS, Mohammadi M: Klotho coreceptors inhibit signaling by paracrine fibroblast growth factor 8 subfamily ligands. Mol Cell Biol 2012;32:1944–1954.

▶3 Miraoui H, Dwyer A, Pitteloud N: Role of fibroblast growth factor signaling in the neuroendocrine control of human reproduction. Mol Cell Endocrinol 2011;346:37–43.

▶4 Falardeau J, Chung WC, Beenken A, Raivio T, Plummer L, Sidis Y, Jacobson-Dickman EE, Eliseenkova AV, Ma J, Dwyer A, Quinton R, Na S, Hall JE, Huot C, Alois N, Pearce SH, Cole LW, Hughes V, Mohammadi M, Tsai P, Pitteloud N: Decreased FGF8 signaling causes deficiency of gonadotropin-releasing hormone in humans and mice. J Clin Invest 2008;118:2822–2831.

▶5 McCabe MJ, Gaston-Massuet C, Tziaferi V, Gregory LC, Alatzoglou KS, Signore M, Pueles E, Gerrelli D, Farooqi IS, Raza J, Walker J, Kavanaugh SI, Tsai PS, Pitteloud N, Martinez-Barbera JP, Dattani MT: Novel FGF8 mutations associated with recessive holoprosencephaly, craniofacial defects, and hypothalamo-pituitary dysfunction. J Clin Endocrinol Metab 2011;96:E1709–E1718.

▶6 Raivio T, Avbelj M, McCabe MJ, Romero CJ, Dwyer AA, Tommiska J, Sykiotis GP, Gregory LC, Diaczok D, Tziaferi V, Elting MW, Padidela R, Plummer L, Martin C, Feng B, Zhang C, Zhou QY, Chen H, Mohammadi M, Quinton R, Sidis Y, Radovick S, Dattani MT, Pitteloud N: Genetic overlap in Kallmann syndrome, combined pituitary hormone deficiency, and septo-optic dysplasia. J Clin Endocrinol Metab 2012;97:E694–E699.

7 Sykiotis GP, Plummer L, Hughes VA, Au M, Durrani S, Nayak-Young S, Dwyer AA, Quinton R, Hall JE, Gusella JF, Seminara SB, Crowley WF Jr, Pitteloud N: Oligogenic basis of isolated gonadotropin-releasing hormone deficiency. Proc Natl Acad Sci USA 2010;107:15140–15144.

8 Trarbach EB, Abreu AP, Silveira LF, Garmes HM, Baptista MT, Teles MG, Costa EM, Mohammadi M, Pitteloud N, Mendonca BB, Latronico AC: Nonsense mutations in FGF8 gene causing different degrees of human gonadotropin-releasing deficiency. J Clin Endocrinol Metab 2010;95:3491–3496.

9 Arauz RF, Solomon BD, Pineda-Alvarez DE, Gropman AL, Parsons JA, Roessler E, Muenke M: A hypomorphic allele in the FGF8 gene contributes to holoprosencephaly and is allelic to gonadotropin-releasing hormone deficiency in humans. Mol Syndromol 2010;1:59–66.

10 Topaloglu AK, Kotan LD: Molecular causes of hypogonadotropic hypogonadism. Curr Opin Obstet Gynecol 2010;22:264–270.

11 Beate K, Joseph N, Nicolas de R, Wolfram K: Genetics of isolated hypogonadotropic hypogonadism: role of GnRH receptor and other genes. Int J Endocrinol 2012;2012:147893.

12 Haraguchi R, Suzuki K, Murakami R, Sakai M, Kamikawa M, Kengaku M, Sekine K, Kawano H, Kato S, Ueno N, Yamada G: Molecular analysis of external genitalia formation: the role of fibroblast growth factor (Fgf) genes during genital tubercle formation. Development 2000;127:2471–2479.

13 Kuzmiak HA, Maquat LE: Applying nonsense-mediated mRNA decay research to the clinic: progress and challenges. Trends Mol Med 2006;12:306–316.

14 Melmed S, Kleinberg D, Ho K: Pituitary physiology and diagnostic evaluation; in Melmed S, Polonsky KS, Larson PR, Kronenberg HM (eds): Williams Textbook of Endocrinology, ed 12. Philadelphia, Saunders, 2011, pp 175–228.

15 Park EJ, Watanabe Y, Smyth G, Miyagawa-Tomita S, Meyers E, Klingensmith J, Camenisch T, Buckingham M, Moon AM: An FGF autocrine loop initiated in second heart field mesoderm regulates morphogenesis at the arterial pole of the heart. Development 2008;135:3599–3610.

16 Wendl T, Adzic D, Schoenebeck JJ, Scholpp S, Brand M, Yelon D, Rohr KB: Early developmental specification of the thyroid gland depends on han-expressing surrounding tissue and on FGF signals. Development 2007;134:2871–2879.

17 Watanabe Y, Miyagawa-Tomita S, Vincent SD, Kelly RG, Moon AM, Buckingham ME: Role of mesodermal FGF8 and FGF10 overlaps in the development of the arterial pole of the heart and pharyngeal arch arteries. Circ Res 2010;106:495–503.

18 Lania G, Zhang Z, Huynh T, Caprio C, Moon AM, Vitelli F, Baldini A: Early thyroid development requires a Tbx1-Fgf8 pathway. Dev Biol 2009;328:109–117.

19 Abu-Issa R, Smyth G, Smoak I, Yamamura K, Meyers EN: Fgf8 is required for pharyngeal arch and cardiovascular development in the mouse. Development 2002;129:4613–4625.

20 Meyers EN, Lewandoski M, Martin GR: An Fgf8 mutant allelic series generated by Cre- and Flp-mediated recombination. Nat Genet 1998;18:136–141.

Mutations in *SERPINB7*, Encoding a Member of the Serine Protease Inhibitor Superfamily, Cause Nagashima-type Palmoplantar Keratosis

Akiharu Kubo,[1,2,3,*] Aiko Shiohama,[1,4] Takashi Sasaki,[1,2,3] Kazuhiko Nakabayashi,[5] Hiroshi Kawasaki,[1] Toru Atsugi,[1,6] Showbu Sato,[1] Atsushi Shimizu,[7] Shuji Mikami,[8] Hideaki Tanizaki,[9] Masaki Uchiyama,[10] Tatsuo Maeda,[10] Taisuke Ito,[11] Jun-ichi Sakabe,[11] Toshio Heike,[12] Torayuki Okuyama,[13] Rika Kosaki,[14] Kenjiro Kosaki,[15] Jun Kudoh,[16] Kenichiro Hata,[5] Akihiro Umezawa,[17] Yoshiki Tokura,[11] Akira Ishiko,[18] Hironori Niizeki,[19] Kenji Kabashima,[9] Yoshihiko Mitsuhashi,[10] and Masayuki Amagai[1,2,4]

"Nagashima-type" palmoplantar keratosis (NPPK) is an autosomal recessive nonsyndromic diffuse palmoplantar keratosis characterized by well-demarcated diffuse hyperkeratosis with redness, expanding on to the dorsal surfaces of the palms and feet and the Achilles tendon area. Hyperkeratosis in NPPK is mild and nonprogressive, differentiating NPPK clinically from Mal de Meleda. We performed whole-exome and/or Sanger sequencing analyses of 13 unrelated NPPK individuals and identified biallelic putative loss-of-function mutations in *SERPINB7*, which encodes a cytoplasmic member of the serine protease inhibitor superfamily. We identified a major causative mutation of c.796C>T (p.Arg266*) as a founder mutation in Japanese and Chinese populations. SERPINB7 was specifically present in the cytoplasm of the stratum granulosum and the stratum corneum (SC) of the epidermis. All of the identified mutants are predicted to cause premature termination upstream of the reactive site, which inhibits the proteases, suggesting a complete loss of the protease inhibitory activity of SERPINB7 in NPPK skin. On exposure of NPPK lesional skin to water, we observed a whitish spongy change in the SC, suggesting enhanced water permeation into the SC due to overactivation of proteases and a resultant loss of integrity of the SC structure. These findings provide an important framework for developing pathogenesis-based therapies for NPPK.

The congenital palmoplantar keratoses (PPKs) are a heterogeneous group of diseases. Phenotypic classification of hereditary PPKs is based mainly on the specific morphology and distribution of the hyperkeratosis, the presence or absence of associated features, and the inheritance pattern and is assisted by additional criteria such as the presence of skin lesions in areas other than the palms and soles, the age at onset of the hyperkeratosis, the severity of the disease process, and histopathological findings.[1]

"Keratosis palmoplantaris Nagashima"[2] or "Nagashima-type" PPK (NPPK)[3] has been proposed as a clinical entity included within the diffuse hereditary PPKs without associated features.[1] A familial case of two siblings was first reported as a distinct clinical type of PPK in 1989.[2,4] Because Nagashima briefly described this type of hereditary PPK in the Japanese literature in 1977,[5] the name "keratosis palmoplantaris Nagashima" was proposed.[2] Although about 20 cases of Japanese individuals with NPPK have been reported in the Japanese literature since then, this clinical entity was not described in detail in the English language literature until 2008.[3]

An autosomal recessive trait has been suggested in NPPK.[2,3] The clinical features of NPPK are characterized by well-demarcated reddish and diffuse palmoplantar hyperkeratosis that extends to the dorsal surfaces of the hands, feet, inner wrists, ankles, and the Achilles tendon area.[2–6] Involvement of the elbows and knees and high frequencies of hyperhidrosis on palms and soles have been noted.[3] Clinical observations revealed no differences between males and females, no seasonal change, and no association with squamous cell carcinoma or any other malignancy. Although mild T cell infiltration in the affected skin area has been reported,[7] the pathophysiology of the skin redness and hyperkeratosis are still uncharacterized.

An autosomal recessive trait, transgressive diffuse hyperkeratosis, and the absence of associated features are also characteristic of Mal de Meleda (MDM [MIM 248300]),[8] PPK Gamborg Nielsen (Norrbotten recessive type PPK [MIM 244850]),[9,10] and acral keratoderma.[11] These other

[1]Department of Dermatology, Keio University School of Medicine, Tokyo 160-8582, Japan; [2]Keio-Maruho Laboratory of Skin Barriology, Keio University School of Medicine, Tokyo 160-8582, Japan; [3]Center for Integrated Medical Research, Keio University School of Medicine, Tokyo 160-8582, Japan; [4]MSD Endowed Program for Allergy Research, Keio University School of Medicine, Tokyo 160-8582, Japan; [5]Department of Maternal-Fetal Biology, National Research Institute for Child Health and Development, Tokyo 157-8535, Japan; [6]KOSÉ Corporation, Tokyo 174-0051, Japan; [7]Department of Molecular Biology, Keio University School of Medicine, Tokyo 160-8582, Japan; [8]Division of Diagnostic Pathology, Keio University Hospital, Tokyo 160-8582, Japan; [9]Department of Dermatology, Kyoto University Graduate School of Medicine, Kyoto 606-8507, Japan; [10]Department of Dermatology, Tokyo Medical University, Tokyo 160-0023, Japan; [11]Department of Dermatology, Hamamatsu University School of Medicine, Hamamatsu 431-3192, Japan; [12]Department of Pediatrics, Kyoto University Graduate School of Medicine, Kyoto 606-8507, Japan; [13]Department of Laboratory Medicine, National Center for Child Health and Development, Tokyo 157-8535, Japan; [14]Department of Clinical Genetics, National Center for Child Health and Development, Tokyo 157-8535, Japan; [15]Center for Medical Genetics, Keio University School of Medicine, Tokyo 160-8582, Japan; [16]Laboratory of Gene Medicine, Keio University School of Medicine, Tokyo 160-8582, Japan; [17]Department of Reproductive Biology, National Research Institute for Child Health and Development, Tokyo 157-8535, Japan; [18]Department of Dermatology, School of Medicine, Toho University, Tokyo 143-8540, Japan; [19]Department of Dermatology, National Center for Child Health and Development, Tokyo 157-8535, Japan
*Correspondence: akiharu@a5.keio.jp
http://dx.doi.org/10.1016/j.ajhg.2013.09.015.

diffuse PPKs show more severe and more progressive features than does NPPK, such as thick hyperkeratosis, leading to flexion contractures (MDM) and constricting bands surrounding the digits (MDM, PPK Gamborg Nielsen, and acral keratoderma), occasionally resulting in spontaneous amputation (MDM and acral keratoderma).[1] NPPK shows only mild and nonprogressive hyperkeratosis and does not show flexion contractures or constricting bands. Thus, NPPK is distinguishable clinically from these other PPKs. Mutations in the coding region of the *SLURP1* (MIM 606119) have been identified in MDM but not in NPPK, suggesting that MDM and NPPK are genetically distinct diseases.[3,12]

To identify gene mutations responsible for NPPK, we performed whole-exome sequencing in three unrelated Japanese NPPK individuals (KDex8 [II-1 of family 1 in Figure 1A], KDex14 [II-2 of family 2], and KDex20 [II-3 of family 3]) who showed the characteristic symptoms of NPPK; Figures 1B and 1C; see Figure S1 available online. Clinical features are summarized in Table 1. The major clinical differentiating points by which we diagnosed these individuals with NPPK among the diverse hereditary PPKs without associated features are summarized in Table 2. The study was conducted after obtaining written informed consent according to the guidelines of the Institutional Review Board of Keio University School of Medicine, National Center for Child Health and Development, Kyoto University, and Tokyo Medical University in accordance with the Helsinki guidelines.

Whole-exome sequencing and data analyses were performed as described previously.[13] Whole-exome sequencing produced approximately 100,000,000 paired reads per sample, approximately 80% of which were mapped to the hs37d5 exon region of the human genome sequence assembly.[14] The average coverage of the exonic region was 87.5×, with more than 93.2% of targeted bases covered at 10× reads. No *SLURP1* mutation (Refseq: NM_020427.2) was identified in any of the three NPPK individuals. A genome informatics study found 693, 677, and 747 allelic variants in three NPPK individuals (KDex8, 14, and 20, respectively), showing a minor allele frequency of less than 1% in the 1092 individuals from the 1000 Genomes Project.[14] Because NPPK is possibly inherited in an autosomal recessive manner,[2,3] the causative mutation was expected to be a homozygous or compound heterozygous variant shared by the affected individuals but absent or found only in a heterozygous manner in the control cohort. Among the identified variants, only mutations in the *SERPINB7* (MIM 603357) fulfilled these requirements, suggesting a causative role in NPPK (Table 1).

SERPINB7 consists of eight exons, with three distinct transcription start sites (exons 1a–c; Figure 2A). The start codon is located within exon 2, and the termination codon within exon 8 (Figure 2A). The *SERPINB7* transcript (RefSeq: NM_001040147.2) encodes a 380 amino-acid protein. Mutations identified by whole-exome sequencing were confirmed by Sanger sequencing by using the primers in Table S1 (Figure 2B). A nonsense mutation encoding a c.796C>T alteration (p.Arg266*) in the last exon of the *SERPINB7* was found in all three NPPK individuals. KDex20 was homozygous for the c.796C>T nonsense mutation. KDex8 was a compound heterozygote of a maternal c.796C>T mutation and a paternal small indel mutation of c.218_219delAGinsTAAACTTTACCT (c.218_219del2ins12) at the end of exon 3, predicted to lead to a premature stop codon (p.Gln73Leufs*17). KDex14 was a compound heterozygote of a maternal c.796C>T mutation and a paternal mutation of c.455-1G>A in the splice acceptor site upstream of exon 6 of *SERPINB7*, which was also predicted to lead to a premature stop codon (p.Gly152Valfs*21) at chromosome 18: 61465837 in the hs37d5 human genome sequence.[14]

To confirm mutations in *SERPINB7* as a cause of NPPK, we analyzed ten additional unrelated NPPK individuals. The clinical manifestations of these individuals are presented in Table 1. Sanger sequencing failed to detect a mutation in *SLURP1* in any of the ten individuals by using methods described previously.[3] When the entire coding region of *SERPINB7* was analyzed by Sanger sequencing with the primers in Table S1, five of the ten individuals were homozygous for the c.796C>T mutation, four were compound heterozygotes of the c.796C>T and c.218_219 del2ins12 mutations, and one was a compound heterozygote of the c.796C>T and c.455-1G>A mutations (Table 1). These results confirmed that mutations in *SERPINB7* are a major cause of NPPK and that c.796C>T and c.218_219 del2ins12 are major mutations for NPPK in a Japanese population.

From our clinical experience, NPPK is much more common than other types of hereditary PPKs in Japan, although no statistical analysis has been reported. NPPK has not been recognized as a clinical entity within PPKs in Western populations, probably because it is rare. Next, we evaluated the variant databases of the cohort of 1,092 individuals in the 1000 Genomes Project[14] to estimate the frequency of *SERPINB7* mutations classified by ethnicity. The nonsense mutation of c.796C>T was identified as an SNP (rs142859678) with a minor allele frequency of 0.4% and found in a heterozygous manner in two of 89 Japanese individuals, four of 97 Han Chinese individuals from Beijing, and two of 100 Han Chinese individuals from southern China. On the other hand, the c.796C>T mutation was not found in any of 806 non-Asian individuals, suggesting that the c.796C>T mutation is a founder mutation causing NPPK in Asian populations. We also found another putative causative mutation, c.336+2T>G (an SNP of rs201433665), in one of 97 Han Chinese individuals from Beijing in a heterozygous manner. Other mutations found in this study were not identified in the 1,092 individuals.

From these results, the prevalence rate of NPPK was estimated as 1.2/10,000 in Japanese populations and 3.1/10,000 in Chinese populations. In contrast, no putative causative mutation (nonsense, missense, insertion,

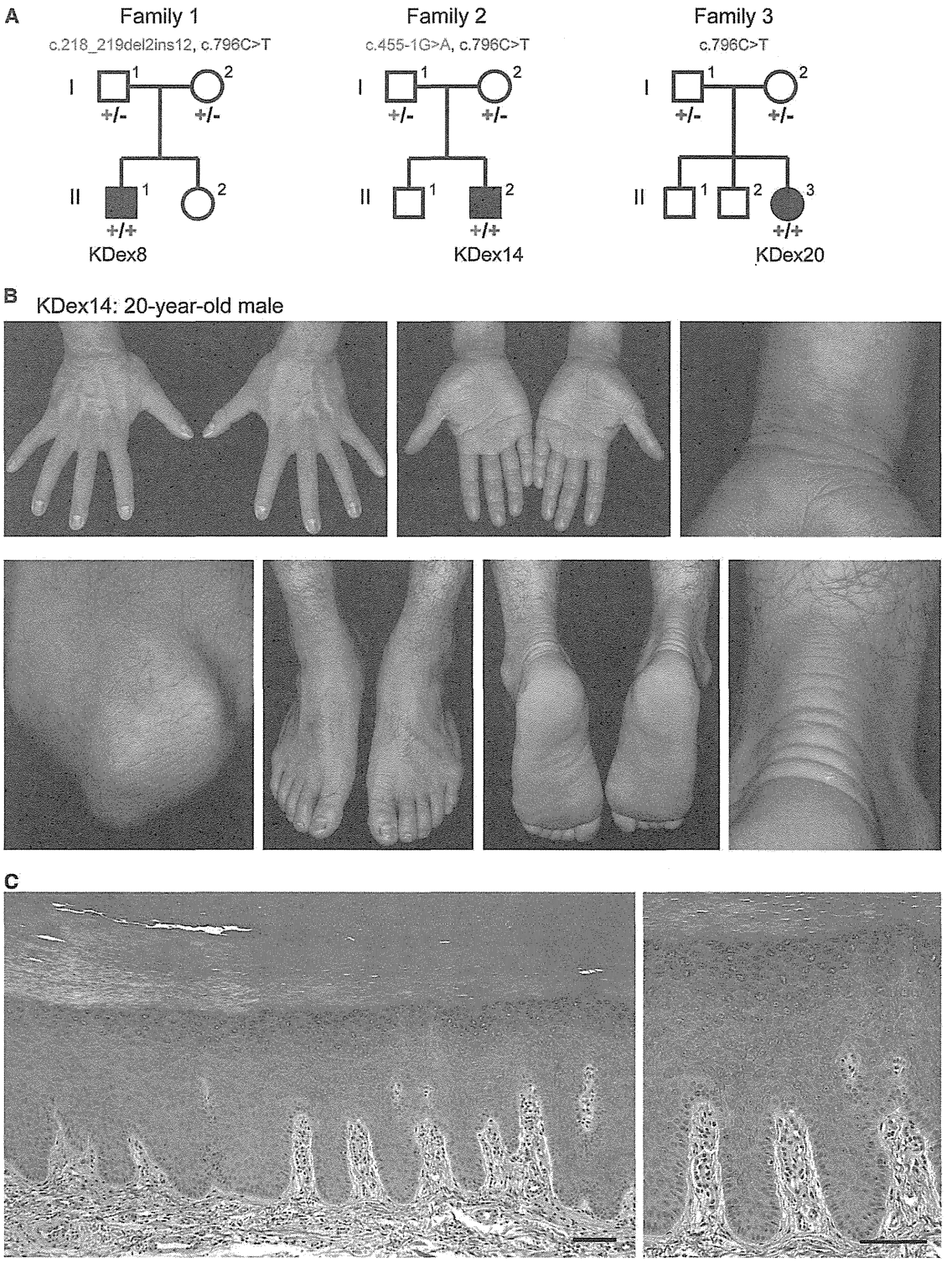

Figure 1. Family Pedigrees and Skin Manifestations of the Probands with NPPK
(A) Pedigrees for the families in which exome sequencing and analyses were performed on the probands (KDex8, KDex14, and KDex20). Segregation of the mutations identified in each pedigree is shown.
(B) Skin manifestations of the proband KDex14.
(C) Hematoxylin and eosin staining of the plantar epidermis of the proband KDex8. Scale bars represent 100 μm.

deletion, or exon-intron boundary mutation) was identified in 806 individuals of non-Asian origin in the 1000 Genomes Project.[14] We further searched causative mutations in European-American and African-American populations by using the NHBLI Exome Variant Server and found only one putative causative mutation, c.309delT in the exon 4 (1 of 12,517 alleles), predicted to lead to a premature stop codon (p.Phe103Leufs*33). Thus, the

Table 1. ***SERPINB7*** **Mutations and Clinical Phenotypes in Individuals with NPPK**

		Allele 1			Allele 2					
Affected Individual	**Gender / Age**	**Base Change**	**Amino Acid Change**	**Segregation**	**Base Change**	**Amino Acid Change**	**Segregation**	**Onset**	**Other Involved Areas**	**Hyperhidrosis**
Homozygous Mutations										
KDex20[a]	F/10	c.796C>T	p.Arg266*	Paternal	c.796C>T	p.Arg266*	Maternal	At birth	Knees	+
KDex55	F/2	c.796C>T	p.Arg266*	Paternal	c.796C>T	p.Arg266*	Maternal	Early infancy	–	–
KDex62	M/31	c.796C>T	p.Arg266*	NA	c.796C>T	p.Arg266*	NA	1 week	Knees	+
KDex72	F/5	c.796C>T	p.Arg266*	Paternal	c.796C>T	p.Arg266*	Maternal	At birth	Knees and elbows	+
KDex79	M/31	c.796C>T	p.Arg266*	NA	c.796C>T	p.Arg266*	NA	At birth	Knees and elbows	+
KDex90	M/14	c.796C>T	p.Arg266*	Paternal	c.796C>T	p.Arg266*	Maternal	9-10 years	Knees and elbows	+
Compound Heterozygous Mutations										
KDex8[a]	M/38	c.796C>T	p.Arg266*	Maternal	c.218_219del2ins12	p.Gln73Leufs*17[b]	Paternal	At birth	Knees and elbows	+
KDex59	F/16	c.796C>T	p.Arg266*	Paternal	c.218_219del2ins12	p.Gln73Leufs*17[b]	Maternal	At birth	–	+
KDex60	F/30	c.796C>T	p.Arg266*	Paternal	c.218_219del2ins12	p.Gln73Leufs*17[b]	Maternal	At birth	Knees	+
KDex64	F/28	c.796C>T	p.Arg266*	Paternal	c.218_219del2ins12	p.Gln73Leufs*17[b]	Maternal	2 years	–	+
KDex66	F/64	c.796C>T	p.Arg266*	NA	c.218_219del2ins12	p.Gln73Leufs*17[b]	NA	Early infancy	–	–
KDex14[a]	M/20	c.796C>T	p.Arg266*	Maternal	c.455-1G>A	p.Gly152Valfs*21[b]	Paternal	At birth	Knees and elbows	+
KDex58	M/51	c.796C>T	p.Arg266*	NA	c.455-1G>A	p.Gly152Valfs*21[b]	NA	5–6 years	Knees and elbows	+

Abbreviations: M, male; F, Female; NA, not available; c.218_219del2ins12, c.218_219delAGinsTAAACTTTACCT.
[a]Whole-exome sequencing performed.
[b]Predicted from genomic sequences.

Table 2. Major Clinical Differentiating Points among Diffuse Hereditary Palmoplantar Keratoses without Associated Features

Types	Vörner[37]	Unna-Thost[38,39]	Greither[40]	Sybert[41]	Bothnian[31]	Mal de Meleda[8]	Nagashima[2,3]	Gamborg Nielsen[9,10]	Acral Keratoderma[11]
Other names	Diffuse Epidermolytic PPK	Diffuse Nonepidermolytic PPK	Progressive PPK			Keratosis Palmoplantaris Transgradiens of Siemens			
MIM number	144200	600962	144200		600231	248300		244850	
Mode of inheritance	AD	AD	AD	AD	AD	AR	AR	AR	AR
Responsible gene	*KRT1*,[42] *KRT9*[43,44]	*KRT1*[45]	*KRT1*[46]	Unknown	*AQP5*[32,33]	*SLURP1*[12]	*SERPINB7*[a]	Unknown	Unknown
Prevalence rate	4.4/100,000 populations in Northern Ireland[47]	Clinical entity in doubt[1,48,49]	Rare	Rare	Rare	Relatively common in the island of Meleda. 1/100,000 in general populations[50]	1.2/10,000 in Japan[a], 3.1/10,000 in China[a]	Rare	Rare
Age of onset	Within the first year of life	Within the first 2 years of life	Ages 8 to 10	Within the first year of life	During childhood, not as early as during the first year of life	Early infancy	Mostly within the first year of life		
Pathologic findings	Epidermolytic hyperkeratosis	Nonepidermolytic	Nonepidermolytic	Nonepidermolytic	Nonepidermolytic	Nonepidermolytic	Nonepidermolytic	Nonepidermolytic	Nonepidermolytic
Hyperkeratosis	Thick	Thick	Thick	Thick	Mild to thick	Severe	Mild	Thick	Thick
Transgrediens	–	–	+	+	+	+	+	+ (1 of 4)	+
Hyperhidrosis	–	–	+	Not described	+	+	+	Not described	Not described
Whitish change upon water exposure	–	–	–	–	+	–	+	–	–
Development on other areas	–	–	Elbows, knees, flexural areas, and Achilles tendon	Natal cleft, groin, elbows, knees, posterior aspects of forearms, and anterior aspects of legs	–	Knees and elbows, perioral erythema, and periorbital erythema	Knees, elbows, and Achilles tendon area	Only knuckle pads on the dorsa of the fingers	Knees, elbows, ankles, Achilles tendon area
Constricting bands	–	–	+	+	–	+	–	+	+
Spontaneous amputation	–	–	+	+	–	Occasionally	–	Not described	+
Flexion contractures	–	–	–	–	–	+	–	–	–

Abbreviations: AD, autosomal dominant inheritance; AR, autosomal recessive inheritance.
[a]This study.

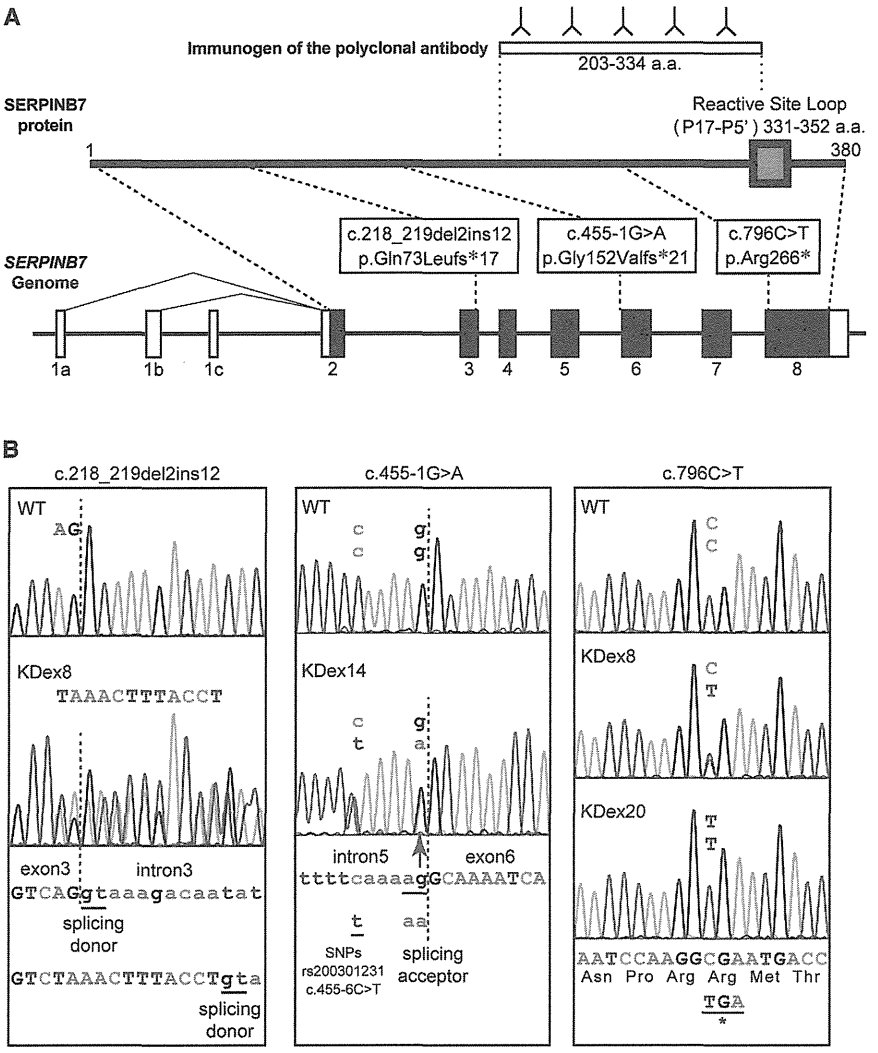

Figure 2. Genomic Organization of *SERPINB7*, Reactive Site Loop for Protease Inhibitory Activity of the SERPINB7 Protein, and Location of NPPK-Causing Mutations

(A) Schematic presentation of the genomic structure of *SERPINB7* (lower) and its encoded protein (middle), SERPINB7. The gray box indicates the reactive site loop indispensable for protease inhibitory activity of SERPINB7. Open and filled boxes indicate exons of untranslated regions and coding regions, respectively. The positions of *SERPINB7* mutations identified in this study are indicated. The immunogen of the anti-SERPINB7 polyclonal antibody is shown at the top.

(B) Heterozygous or homozygous mutated sequences of affected individuals (KDex8, KDex14, and KDex20) compared with the corresponding wild-type sequences. The base and amino acid sequences are shown. The intron-exon junctions are shown with red dotted lines. Intron and exon sequences are shown in lower case and upper case, respectively.

Abbreviations are as follows: c.218_219 del2ins12, c.218_219delAGinsTAAACTTT ACCT.

prevalence rate of NPPK in non-Asian populations was ~0.5/100,000,000. These results well explain why NPPK is so common in PPKs in Japanese populations but has not been reported from non-Asian countries.

Serpins were originally identified as serine protease inhibitors. Serpin molecules are evolutionarily old because even bacteria and Archaea possess them.[15–17] Most serpins identified to date possess protease inhibitory activity, although their protease targets are now known not to be restricted to serine proteases.[16,17] Serpins form covalent complexes with target proteases to inhibit protease activity irreversibly. Human serpins have been divided into nine clades (A–I) by phylogenetic analyses.[15,18] Several congenital diseases have been reported to be caused by deficiencies in the protease inhibitory function of serpins—for example, plasminogen activator inhibitor-1 deficiency (MIM 613329) with mutations in *SERPINE1* (MIM 173360)[19]—or to be caused by polymerization and accumulation of mutated serpins, for example, familial encephalopathy with neuroserpin inclusion bodies (MIM 604218) with mutations in *SERPINI1* (MIM 602445).[20]

SERPINB7 is located on chromosome 18q21.3, forming a cluster of clade-B serpin genes.[18] Clade-B serpins are intracellular serpins, possibly protecting cells from exogenous and endogenous protease-mediated injury.[18] The protease-inhibitory activity of serpins is dependent on the reactive site loop to form a covalent bond with target proteases.[16] The center of the reactive site loop (P1–P1′) is located at amino acids 347–348 of SERPINB7,[16] and the entire region of the reactive site loop (P17–P5′, corresponding to the amino acid region 331–352 of SERPINB7) is predicted to be absent in all of the mutant proteins (Figure 2A). Thus, all of the mutations identified in this study presumably result in a complete loss of the protease inhibitory activity of SERPINB7.

SERPINB7 was originally described as being expressed in kidney mesangial cells and was named *MEGSIN*.[21] However, no renal manifestation has been identified in NPPK individuals. A recent report using a bacterial artificial chromosome transgene expressing Cre in mice under the control of *Serpinb7* regulatory elements showed specific expression of Cre in cornified stratified epithelial cells, but not in kidney mesangial cells,[22] suggesting that *Serpinb7* might be specifically expressed in epidermal keratinocytes in mice. Thus, we next analyzed the expression of *SERPINB7* in human skin. We used a commercial polyclonal antibody (HPA024200; Sigma-Aldrich) raised against a peptide corresponding to the amino acid 203–334 region of human SERPINB7 (Figure 2A). To characterize

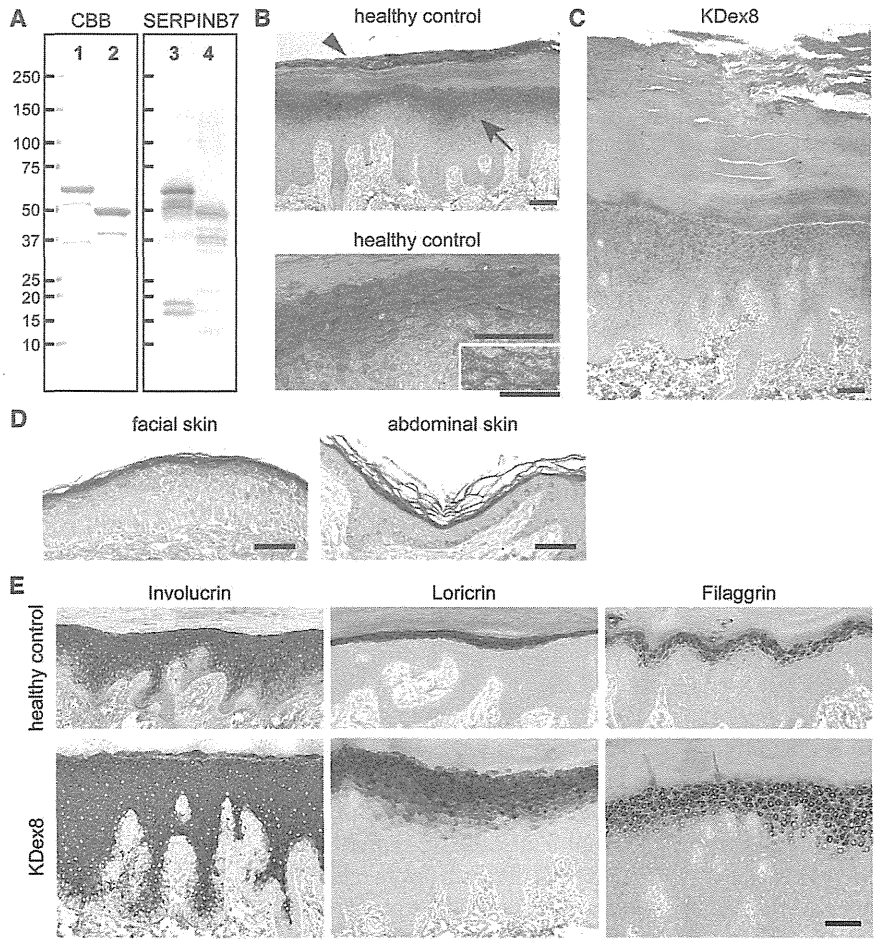

Figure 3. SERPINB7 Localization in the Epidermis and Immunohistochemical Analysis of the Affected Skin

(A) Investigation of the anti-SERPINB7 antibody. GST-fused recombinant full-length human SERPINB7 (lanes 1 and 3) and GST-fused recombinant p.Arg266* mutant (lanes 2 and 4) were analyzed by electrophoresis with Coomassie Brilliant Blue staining (lanes 1 and 2) or with immunoblotting with the anti-SERPINB7 rabbit polyclonal antibody (lanes 3 and 4). Scale bars indicate molecular weights (kDa).

(B) Immunohistochemistry of SERPINB7 in plantar skin of a healthy control. Upper panel shows SERPINB7 in the stratum granulosum (arrow) and in the upper part of the stratum corneum (arrowhead). Lower panel shows the intracellular distribution of SERPINB7 in the stratum granulosum. Scale bars represent 100 μm. Inset in the lower panel shows stratum granulosum cells and intercellular spaces at higher magnification (scale bar represents 50 μm).

(C) Immunohistochemistry of SERPINB7 in the hyperkeratotic plantar skin of NPPK individual of KDex8. Scale bar represents 100 μm.

(D) Immunohistochemistry of SERPINB7 in facial and abdominal skin sections of a healthy control. Scale bars represent 100 μm.

(E) Immunohistochemistry of epidermal differentiation-related proteins in plantar skin of a healthy control (upper panels) and a NPPK individual (KDex8; lower panels). Scale bar represents 100 μm.

the antibody, we performed immunoblotting against GST-fused full-length human SERPINB7 and GST-fused p.Arg266* mutant that were produced in *Escherichia coli* BL21(DE3) by using the pGEX 5X-1 vector (GE Healthcare) in inclusion bodies and purified by washing with 1% Triton X-100 and 4 M urea. The purified proteins showed molecular weights of ~62 kDa and ~50 kDa in SDS-PAGE analysis, respectively (Figure 3A). In immunoblotting analysis, the anti-SERPINB7 antibody recognized both the GST-fused full-length SERPINB7 and GST-fused p.Arg266* mutant (Figure 3A). The immunosignals for the full-length SERPINB7 were stronger than those for the truncated p.Arg266* mutant, suggesting that this polyclonal antibody includes antibodies against peptides corresponding to both the amino acid 203–265 region and the 266–334 region of human SERPINB7 (Figure 2A).

Using this antibody, we performed an immunohistochemical analysis of paraffin wax-embedded sections of healthy human skin and NPPK skin, with antigen retrieval with 15 min boiling in a microwave oven in 100 mM Tris-HCl and 1 mM EDTA buffer (pH 9.0), immunosignal detection with ImmPRESS kit and NovaRed substrates (Vector Laboratories), and counterstaining with methyl green (Wako Pure Chemical). The immunosignals of the antibody were specifically detected from the stratum granulosum and from the upper part of the SC in healthy control plantar skin (Figure 3B). No signal was detected from the lower part of the SC, probably because the tightly packed intracorneocyte proteinaceous structure prevents access of the antibody to the antigen. When the stratum granulosum was observed at higher magnification, signals were observed in the cytoplasm, with a mild concentration to the apical side of the stratum granulosum cells (Figure 3B). In NPPK individuals, the immunosignals of the stratum granulosum and the SC were markedly diminished (KDex8, a compound heterozygote of the c.796C>T and c.218_219del2ins12 mutations; Figure 3C. For other affected individuals, data are not shown or skin biopsies were not performed). Thus, the immunosignals observed in healthy control plantar skin were considered to represent the distribution of SERPINB7. Some nuclear staining was observed in both the healthy control skin and the NPPK skin, which was considered to be nonspecific background (Figures 3B and 3C). Weak cytoplasmic immunosignals were observed in the NPPK skin, which were considered to be due to the p.Arg266* mutant of SERPINB7 or nonspecific background (Figure 3C).

To clarify whether *SERPINB7* expression was limited to the palmoplantar area of the skin, we immunostained facial and abdominal skin sections of healthy controls. SERPINB7 immunosignals were specifically detected from the stratum granulosum and the SC in facial and abdominal epidermis